

QCD Results from HERA

D. BRITZGER for the H1 and ZEUS Collaborations
DESY, Notkestr. 85, 22607 Hamburg, Germany

New results on the measurements of the hadronic final state in neutral-current deep-inelastic scattering at HERA are presented. A combination of reduced charm and beauty cross sections is presented and the masses of the heavy quarks are determined to $m_c = 1290^{(+78)}_{(-53)}$ MeV and $m_b = 4049^{(+138)}_{(-118)}$ MeV. The measurement of the production of prompt photons accompanied by a jet provides a precise test of QCD predictions. Measurements of jet production cross sections are presented and compared for the first time to next-to-next-to-leading order predictions (NNLO). The strong coupling constant is determined from inclusive jet and dijet production cross sections using NNLO predictions to $\alpha_s(M_Z) = 0.1157(6)_{\text{exp}}^{(+31)}_{(-26)\text{th}}$.

1 Introduction

At the HERA collider electrons or positrons were collided with protons at a centre-of-mass energy of 319 GeV. The two multi-purpose experiments H1 and ZEUS collected data until 2007 with an integrated luminosity of about 0.5 fb^{-1} per experiment. The exploration of the hadronic final state in neutral-current (NC) DIS events, such as the study of jets, heavy quarks or photons produced in these events, provides precise constraints on QCD parameters.

2 Charm and Beauty Cross Sections

Multiple measurements of open charm and beauty production cross sections have been performed by the H1 and ZEUS experiments during different data-taking periods and using different tagging techniques. A previous combination¹ of charm cross sections is extended, taking new data into account, and also beauty cross sections are combined for the first time². This provides a consistent data set of reduced charm and beauty cross sections, $\sigma_{\text{red}}^{c\bar{c}}$ and $\sigma_{\text{red}}^{b\bar{b}}$, in the kinematic range of photon virtuality $2.5 < Q^2 < 2000 \text{ GeV}^2$ and Bjorken- x of $3 \cdot 10^{-5} < x_{\text{Bj}} < 5 \cdot 10^{-2}$.

The reduced cross sections which are input to the combination are obtained by extrapolating the visible cross sections to the nearest point of a (x_{Bj}, Q^2) grid using NLO predictions by the HVQDIS program. The combination algorithm accounts for all correlations of the uncertainties and in total 209 charm and 57 beauty measurements are combined simultaneously to 52 reduced charm and 27 reduced beauty cross sections. The combination yields a value of $\chi^2 = 149$ for 187 degrees of freedom, thus indicating good consistency of the individual data. The combined data have significantly reduced uncertainties. The data are compared to NLO predictions using the HERAPDF2.0FF3A or the ABM11 PDF sets, as well as to approximate NNLO predictions using the ABMP16 PDF set in figure 1. All predictions are found to give a reasonable description of the data, with only small differences between the studied predictions.

A QCD analysis of the combined charm and beauty reduced cross sections together with the combined HERA inclusive DIS data³ is performed, where the predictions are calculated by the QCDNUM and OPENQCDRAD programs in NLO accuracy. The methodology follows closely the approach of HERAPDF2.0FF3A³, employing the fixed-flavour scheme with three active flavours at all scales, but in addition the masses of the charm and beauty quarks are free

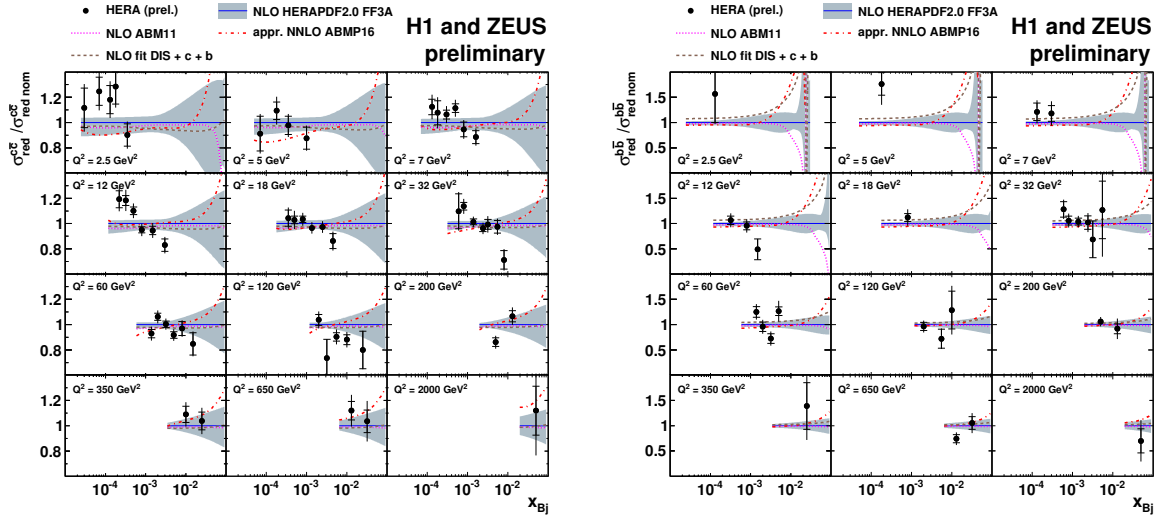


Figure 1 – Combined reduced charm (left) and beauty cross sections (right) as a function of x_{Bj} for given values of Q^2 , displayed as ratios to NLO predictions using HERAPDF2.0FF3A.

parameters to the fit. In this fit the running charm and beauty quark masses are determined to

$$\begin{aligned} m_c(m_c) &= 1290^{(+46)}_{(-41)}{}_{\text{exp}} \, ^{(+62)}_{(-14)}{}_{\text{mod}} \, ^{(+7)}_{(-31)}{}_{\text{par}} \text{ MeV} \text{ and} \\ m_b(m_b) &= 4049^{(+104)}_{(-109)}{}_{\text{exp}} \, ^{(+90)}_{(-32)}{}_{\text{mod}} \, ^{(+1)}_{(-31)}{}_{\text{par}} \text{ MeV} , \end{aligned} \quad (1)$$

where the uncertainties indicate experimental uncertainties, model uncertainties (mod), mainly dominated by scale variations by factors of 2, and parameterisation uncertainties (par), which are determined using fits with extended parameterisations of the PDFs. The inclusive DIS data alone cannot reliably constrain the quark masses. The results are consistent with other determinations.

3 Isolated photons accompanied by jets in DIS

The production of isolated photons in events with at least one jet is measured in NC DIS in the kinematic region of $10 < Q^2 < 350 \text{ GeV}^2$. Photons were measured with transverse energy $4 < E_T^\gamma < 15 \text{ GeV}$ and pseudorapidity $-0.7 < \eta^\gamma < 0.9$, and jets with $2.5 < E_T^{\text{jet}} < 35 \text{ GeV}$ and $-1.5 < \eta^\gamma < 1.8$. The analysis complements earlier measurements of isolated photon production in NC DIS⁴, and now differential cross sections as functions x_γ , x_p , $\Delta\eta$, $\Delta\phi$, $\Delta\eta_{e,\gamma}$ and $\Delta\phi_{e,\gamma}$ are provided, where the observables denote the fraction of the incoming photon energy that is given to the photon and the jet, the fraction of proton energy taken by the interacting parton, and the azimuthal angles or rapidity differences between the photon and the jet or the scattered lepton, respectively. The cross sections are compared to Monte Carlo predictions by Djangoh+Pythia, where the photons radiated off a quark line are scaled by a factor of 1.6. These predictions provide a good description of the studied distributions⁵, as exemplarily displayed in figure 2. The cross sections are further compared to predictions based on the k_T factorisation method, which appear to have some problems in describing all measured distributions equally well.

4 Jet cross sections in DIS

Cross sections for jet production are measured in NC DIS in the Breit frame and exhibit a direct sensitivity to the strong coupling constant and to the gluon content of the proton. New measurements of jet production cross sections in NC DIS have been performed in the kinematic region $5.5 < Q^2 < 80 \text{ GeV}$ and inelasticity $0.2 < y < 0.6$. These are inclusive jet cross sections

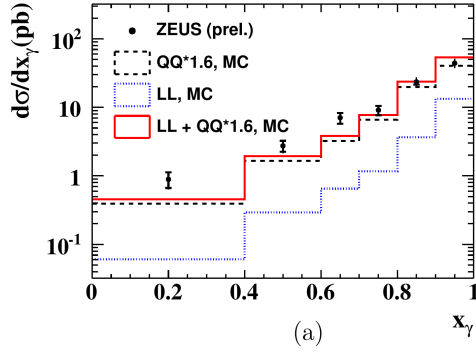


Figure 2 – Differential cross sections for the production of photons accompanied by a jet in NC DIS as a function of fraction of the incoming photon energy that is given to the photon and the jet, x_γ , compared to MC predictions by Djangoh+Pythia.

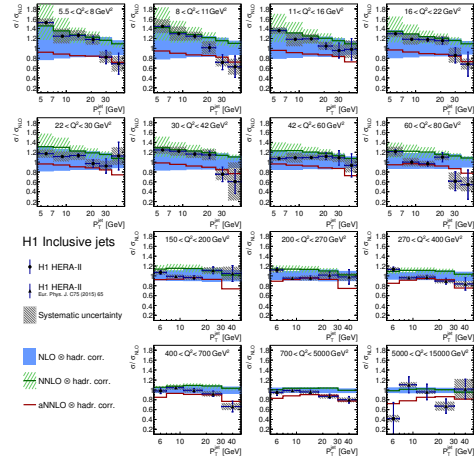


Figure 3 – Inclusive jet cross sections in NC DIS in comparison to NLO, approximate NLO and full NNLO predictions.

measured as a function of Q^2 and jet transverse momentum, P_T^{jet} , as well as dijet and trijet cross sections measured as functions of Q^2 and the average P_T^{jet} of the two or three leading jets⁶. Furthermore, the kinematic range of an earlier measurement of inclusive jet cross sections⁷ at higher values of Q^2 is extended to lower values of P_T^{jet} . The data are compared to NLO, to approximate NNLO and to next-to-next-to-leading order (NNLO) predictions⁸, whenever available. The ratio of inclusive jet cross sections to NLO calculations together with other predictions is displayed in figure 3. The predictions are in general found in good agreement with the data within the experimental and theoretical uncertainties. The NNLO predictions improve significantly the description of inclusive jet and dijet cross sections as compared to NLO predictions in particular at lower scales and they also exhibit reduced scale uncertainties. Measurements of jet cross sections normalised to the inclusive NC DIS cross section in the respective Q^2 interval further improve the experimental precision, since experimental uncertainties cancel partially.

5 Strong coupling constant at NNLO from jet cross sections

The strong coupling constant $\alpha_s(M_Z)$ is determined in a fit of NNLO predictions⁸ to inclusive jet and dijet cross sections measured by the H1 experiment during different data taking periods and different center-of-mass energies⁹. Altogether five data sets of inclusive jet cross sections and four data sets of dijet cross sections are considered and the data covers a range of momentum transfer of $5.5 < Q^2 < 15\,000 \text{ GeV}^2$ and jet transverse momenta of $P_T^{\text{jet}} > 4.5 \text{ GeV}$. Jets are defined by the k_t jet-algorithm with a parameter $R = 1$ and are contained within the pseudorapidity range $-1 < \eta_{\text{lab}}^{\text{jet}} < 2.5$. The α_s -extraction methodology accounts for the α_s -dependence of the hard coefficients, as well as the α_s -dependence of the PDFs⁹. The latter is predicted by the factorisation theorem and it is taken as such into account in the fit. This provides an increased sensitivity to α_s at lower scales, but a decreased sensitivity at higher scales.

Values of $\alpha_s(M_Z)$ are determined in fits to the individual data sets, and in fits to all inclusive jet and dijet measurements as displayed in figure 4. These values are found to be consistent. The value of $\alpha_s(M_Z)$ determined in a fit to inclusive jet and dijet cross sections is found to be

$$\alpha_s(M_Z) = 0.1157 (6)_{\text{exp}} (3)_{\text{had}} (6)_{\text{PDF}} (12)_{\text{PDF}\alpha_s} (2)_{\text{PDFset}} \left(\begin{smallmatrix} +27 \\ -21 \end{smallmatrix} \right)_{\text{scale}} ,$$

where uncertainties on the PDF, the choice of the PDF set (PDFset), the value of $\alpha_s(M_Z)$ as input to the PDF extraction (PDF α_s), the uncertainty on the hadronisation correction, and uncertainties due to scale variations by factors of 2, are considered. The value of $\alpha_s(M_Z)$ is consistent with the world average value of $\alpha_s(M_Z) = 0.1181 (11)$. The dominating uncertainty arises from scale variations of the NNLO predictions.

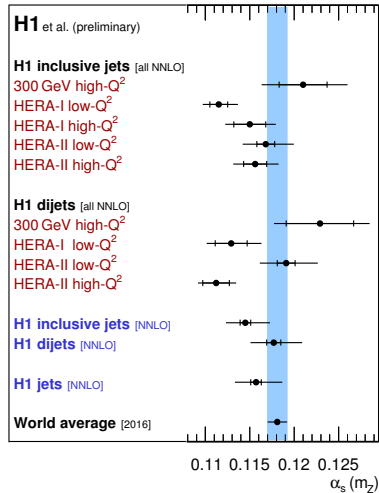


Figure 4 – Values of the strong coupling constant, $\alpha_s(M_Z)$, determined in NNLO accuracy in fits to H1 jet cross section measurements.

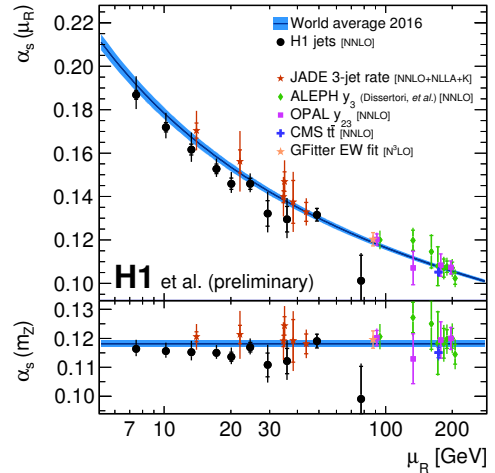


Figure 5 – Results for $\alpha_s(M_Z)$ in NNLO for fits to data points at similar scales in comparison to values from other experiments and processes.

The running of the strong coupling constant is determined by repeating the fits to groups of data points at similar scales. The results are displayed in figure 5 and compared to other extractions in at least NNLO accuracy. Good agreement with the QCD expectation and other determinations is found.

6 Summary and conclusions

Several years after ending of data taking at the HERA accelerator the H1 and ZEUS experiments have transformed their analysis frameworks into a long-term usable computational environment and provide new measurements and also combinations of previously published results. New theoretical developments, such as full next-to-next-to-leading order calculations for jet production, can thus be explored together with new data and precision QCD results are obtained, such as precision determinations of the strong coupling constant, $\alpha_s(M_Z)$, or the masses of heavy quarks.

References

1. H. Abramowicz et al. [H1 and ZEUS Collaborations], *Eur.Phys.J.* C73 (2013) 2, 2311, [arXiv:1211.1182].
2. H1 and ZEUS Collaborations, H1 and ZEUS preliminary report, H1prelim-17-071, ZEUS-prel-17-01 (2017).
3. H. Abramowicz et al. [H1 and ZEUS Collaborations], *Eur.Phys.J.* C75 (2015) 12, 580, [arXiv:1506.06042].
4. S. Chekanov et al. [ZEUS Collaboration], *Phys. Lett.* B687 (2010) 16;
H. Abramowicz et al. [ZEUS Collaboration], *Phys.Lett.* B715 (2012) 88, [arXiv:1206.2270].
5. ZEUS Collaboration, ZEUS preliminary report, ZEUS-prel-16-001 (2016).
6. V. Andreev et al. [H1 Collaboration], *Eur.Phys.J.* C77 (2017) 4, 215, [arxiv:1611.03421].
7. V. Andreev et al. [H1 Collaboration], *Eur.Phys.J.* C75 (2015) 2, 65, [arxiv:1406.4709].
8. J. Currie et al., *Phys.Rev.Lett.* 117 (2016) 4, 042001, [arXiv:1606.03991];
J. Currie et al., [arXiv:1703.05977]; J. Niehues et al., these proceedings.
9. H1 Collaboration and V. Bertone et al., H1 preliminary report, H1prelim-17-031 (2017).